JVI Journals.ASM.org

A Unique Nodavirus with Novel Features: Mosinovirus Expresses Two Subgenomic RNAs, a Capsid Gene of Unknown Origin, and a Suppressor of the Antiviral RNA Interference Pathway

Susan Schuster,[a] Florian Zirkel,[b] Andreas Kurth,[c] Koen W. R. van Cleef,[a] Christian Drosten,[b] Ronald P. van Rij,[a] Sandra Junglen[b]

Department of Medical Microbiology, Radboud University Nijmegen Medical Centre, Radboud Institute for Molecular Life Sciences, Nijmegen, The Netherlands[a]; Institute of Virology, University of Bonn Medical Centre, Bonn, Germany[b]; Center for Biological Threats and Special Pathogens, Robert Koch-Institute, Berlin, Germany[c]

ABSTRACT

Insects are a reservoir for many known and novel viruses. We discovered an unknown virus, tentatively named mosinovirus (MoNV), in mosquitoes from a tropical rainforest region in Côte d'Ivoire. The MoNV genome consists of two segments of positive-sense RNA of 2,972 nucleotides (nt) (RNA 1) and 1,801 nt (RNA 2). Its putative RNA-dependent RNA polymerase shares 43% amino acid identity with its closest relative, that of the Pariacoto virus (family *Nodaviridae*). Unexpectedly, for the putative capsid protein, maximal pairwise identity of 16% to Lake Sinai virus 2, an unclassified virus with a nonsegmented RNA genome, was found. Moreover, MoNV virions are nonenveloped and about 50 nm in diameter, larger than any of the known nodaviruses. Mature MoNV virions contain capsid proteins of ~56 kDa, which do not seem to be cleaved from a longer precursor. Northern blot analyses revealed that MoNV expresses two subgenomic RNAs of 580 nt (RNA 3) and 292 nt (RNA 4). RNA 4 encodes a viral suppressor of RNA interference (RNAi) that shares its mechanism with the B2 RNAi suppressor protein of other nodaviruses despite lacking recognizable similarity to these proteins. MoNV B2 binds long double-stranded RNA (dsRNA) and, accordingly, inhibits Dicer-2-mediated processing of dsRNA into small interfering RNAs (siRNAs). Phylogenetic analyses indicate that MoNV is a novel member of the family *Nodaviridae* that acquired its capsid gene via reassortment from an unknown, distantly related virus beyond the family level.

IMPORTANCE

The identification of novel viruses provides important information about virus evolution and diversity. Here, we describe an unknown unique nodavirus in mosquitoes, named mosinovirus (MoNV). MoNV was classified as a nodavirus based on its genome organization and on phylogenetic analyses of the RNA-dependent RNA polymerase. Notably, its capsid gene was acquired from an unknown virus with a distant relationship to nodaviruses. Another remarkable feature of MoNV is that, unlike other nodaviruses, it expresses two subgenomic RNAs (sgRNAs). One of the sgRNAs expresses a protein that counteracts antiviral defense of its mosquito host, whereas the function of the other sgRNA remains unknown. Our results show that complete genome segments can be exchanged beyond the species level and suggest that insects harbor a large repertoire of exceptional viruses.

The ongoing identification of novel viruses in insects illustrates the fact that our understanding of virus diversity is far from complete. The characterization of novel viruses provides important new insights into genome organization and replication strategies. For example, a new nidovirus family named *Mesoniviridae* has recently been identified in mosquitoes (1, 2), and it uses a unique mechanism to generate subgenomic RNAs and express the spike glycoprotein (3). Another example is the discovery of clades of putatively insect-specific bunyaviruses with less complex genomes than vertebrate-infecting bunyaviruses, suggesting that they encode only the basic genes necessary for virus maintenance in insects (4, 5). Furthermore, novel viruses with a bipartite positive-sense RNA genome, chronic bee paralysis virus (CBPV) and anopheline-associated C virus (AACV), were identified in bees and mosquitoes, respectively (6, 7). These viruses are distantly related to members of the family *Nodaviridae* and may comprise a novel virus family. Lake Sinai virus 1 (LSV1) and LSV2 are two novel monopartite, positive-sense RNA viruses identified in honeybees (8). They are distantly related to members of the monopartite family *Tombusviridae*, as well as to CBPV and AACV, suggesting that they also belong to a novel virus family.

The family *Nodaviridae* contains two established genera, *Alphanodavirus* and *Betanodavirus*, which infect insects and fish, respectively. Although alphanodaviruses naturally infect only insects, their RNAs can replicate in vertebrate (9, 10), plant (11), and yeast (12) cells. Betanodaviruses cause significant problems in marine fish aquacultures worldwide (13). Recently, three further clades of unclassified nodaviruses infecting moths and butterflies (14–17), nematodes (18), and prawns (19) were identified. These clades are only distantly related to the alpha- and betanodaviruses (also see below), suggesting that they may represent new genera within the *Nodaviridae*. These findings suggest that the *Nodaviridae* family comprises members with wide distribution in metazoans.

Received 21 July 2014 **Accepted** 2 September 2014
Published ahead of print 10 September 2014
Editor: D. S. Lyles
Address correspondence to Ronald P. van Rij, R.vanRij@ncmls.ru.nl, or Sandra Junglen, junglen@virology-bonn.de.
S.S. and F.Z. contributed equally to this work.

doi:10.1128/JVI.02144-14

The nonenveloped nodavirus virions are ~30 nm in diameter and contain a bipartite positive-sense RNA genome (for a review, see reference 20). Both RNA segments are 5′ capped, while their 3′ ends lack a poly(A) tail. RNA 1 (~3 kb) encodes protein A (~102 kDa), the RNA-dependent RNA polymerase (RdRp). RNA 2 (~1.5 kb) encodes the capsid precursor protein α, which is autocatalytically cleaved into the viral capsid proteins β (38 kDa) and γ (5 kDa) during particle maturation of alphanodaviruses (21). Autocatalytic cleavage of the capsid protein is required for virion stability and infectivity of alphanodaviruses (22) but does not occur in betanodaviruses (23). Other unclassified nodaviruses, like Wuhan nodavirus (WhNV), contain a major and a minor capsid protein of 40 and 44 kDa, respectively (24).

During nodavirus RNA replication, a subgenomic RNA, RNA 3, is synthesized from the 3′ terminus of RNA 1. RNA 3 encodes one or two proteins (B1 and B2) in overlapping ORFs (25–27). The B2 protein is essential for evading antiviral RNA interference (RNAi) responses (28–32). RNAi is a crucial antiviral defense system in insects (33, 34). Antiviral RNAi is activated by viral double-stranded RNA (dsRNA), which is processed into viral small interfering RNAs (vsiRNAs) of 21 nucleotides (nt) by the RNase Dicer-2 (Dcr-2) (28, 29, 35–45). The current model proposes that these vsiRNAs are loaded onto Argonaute-2 (AGO2) in the RNA-induced silencing complex (RISC) to guide the recognition and cleavage of viral target RNA by AGO2, thereby restricting viral replication (29, 33, 37, 38, 46–48). Indeed, fruit flies deficient in Dicer-2, its cofactor R2D2, and AGO2 are hypersensitive to virus infection and support higher levels of viral replication than wild-type flies (32, 35–38, 48, 49). Similarly, knockdown of crucial RNAi genes, such as Dcr-2 and AGO2, in mosquitoes results in higher titers of different viruses (50–52).

Nodaviruses are an attractive system for studying antiviral RNAi responses and viral counterdefense mechanisms. For example, using Flock House virus (FHV) as a model, it was shown for the first time that insect viruses may encode virus-encoded suppressors of RNAi (VSRs) (30). FHV B2 interferes with multiple steps of the RNAi pathway. B2 has dsRNA binding activity, and it was proposed that this prevents Dicer from processing dsRNA into siRNAs (53–55). In addition, FHV B2 binds to Dcr-2, which might affect its processing activity (56). Moreover, B2 binds siRNAs, thereby preventing their incorporation into RISC (53–55). Importantly, a FHV mutant that lacks B2 expression (ΔB2) has severe replication defects in RNAi-competent hosts but not in RNAi-deficient systems, indicating that suppression of antiviral RNAi is the main function of B2 (28, 29, 32). Members of other insect virus families also encode VSRs. For example, Drosophila C virus 1A inhibits RNAi by binding long dsRNA (48), Drosophila X virus and Culex Y virus VP3 have dsRNA and siRNA binding activity (57), whereas Nora virus VP1 and cricket paralysis virus (CrPV) 1A suppress RNAi by antagonizing the catalytic activity of AGO2 (32, 47, 58, 59).

To gain more insight into virus-mosquito interactions, we surveyed wild-caught mosquitoes for unknown viruses. Here, we report the isolation of an atypical nodavirus from mosquitoes, tentatively named mosinovirus (MoNV, for mosquito nodavirus). MoNV was sampled in a tropical rainforest region in Côte d'Ivoire. We analyzed the complete genome, inferred the phylogenetic relationships, investigated virion morphology and viral structural proteins, characterized the subgenomic RNAs, and tested the ability of MoNV to suppress the host RNAi response.

MATERIALS AND METHODS

Cell culture. *Drosophila* S2 cells (Invitrogen) and S2 R+ cells (60) were cultured at 25°C in Schneider's medium (Invitrogen) supplemented with 10% heat-inactivated fetal calf serum (PAA), 50 U/ml penicillin, and 50 mg/ml streptomycin (Invitrogen). *Aedes albopictus*-derived U4.4 (61) and C6/36 (62) cells were cultured at 28°C in Leibovitz's medium (Invitrogen) supplemented with 10% heat-inactivated fetal calf serum, 50 U/ml penicillin, 50 mg/ml streptomycin (Invitrogen), 1% modified Eagle medium (MEM) with nonessential amino acids (Invitrogen), and 2% tryptose phosphate broth solution (Sigma-Aldrich). Vero E6 and BHK-J cells were cultured at 37°C with 5% CO_2 in Dulbecco's modified Eagle medium (DMEM) (Invitrogen) supplemented with 10% fetal calf serum and 2% L-glutamine.

Virus isolation, purification, and protein analyses. Virus isolation from mosquitoes was performed in C6/36 cells as described previously (63, 64). Briefly, mosquitoes were stored in liquid nitrogen in the field and at −80°C in the laboratory until further analysis. For virus isolation trials, mosquitoes were pooled and homogenized in DMEM without additives. Aliquots were cleared from debris by centrifugation, and subconfluent cells seeded were infected with supernatants in 24-well plates. Cells were monitored daily for signs of cytopathic effects (CPE). An aliquot of the supernatant (1:10 dilution) was used to infect fresh cells when 80% of the cells showed CPE. A stock of the third passage of MoNV (isolate C36/CI/2004) was prepared. Virus titers were determined by 50% tissue culture infective dose ($TCID_{50}$) titration in C6/36 cells. Virus-positive wells were identified by observation of cytopathic effects. Virions were concentrated from the supernatant of one T175 flask of infected C6/36 cells by ultracentrifugation through a 36% (wt/vol) sucrose cushion. The virus pellet was resuspended in 200 μl phosphate-buffered saline (PBS) at 4°C overnight (63). For the analyses of the protein content of viral particles, MoNV virions were purified by gradient ultracentrifugation on a continuous gradient of 1 to 2 M sucrose in 0.001 M Tris-HCl-4 mM EDTA, and proteins were analyzed by SDS-PAGE as described previously (5).

Electron microscopy. For electron microscopy (EM), an aliquot of purified, concentrated virus (10 μl) was fixed with 2% paraformaldehyde and processed for direct negative-staining electron microscopy (65, 66). The sample was contrasted with 1% uranyl acetate and examined by transmission electron microscopy.

Virus growth kinetics. C6/36 and U4.4 cells were infected at an multiplicity of infection (MOI) of 0.001 in duplicate in two independent experiments as described previously (1). Aliquots of cell culture supernatant were harvested at 1 h postinfection (hpi) and then every 24 hpi for a period of 5 days. Vero E6 and BHK-J cells were infected at MOIs of 0.01 and 0.1 in duplicate, and aliquots of cell culture supernatant were harvested at 1 hpi and 7 days postinfection (dpi). RNA was extracted using the NucleoSpin RNA virus kit (Macherey-Nagel), and cDNA was synthesized using the SuperScript III RT system (Life Technologies) and random hexamer primers. Viral genome copy numbers were quantified by real-time RT-PCR using the primers MoNV-F (5′-GAGTACGTCGAGGCGGTGAT-3′) and MoNV-R (5′-CGCGGATGGTGTCATTAGTG-3′) and the probe MoNV-TM (5′-6-carboxyfluorescein [FAM]-AGCCGCCCCGTTAAGC TACGCC-TQ2).

Unbiased ultradeep sequencing. Deep sequencing was performed using the GS-Junior platform (Roche) following the manufacturer's instructions. Briefly, RNA was extracted from purified virus pellets using TRIzol LS reagent (Life Technologies). Double-stranded cDNA was generated using a cDNA synthesis system (Roche) with random hexamer primers. The cDNA was fragmented via liquid nitrogen nebulization, followed by adapter ligation, emulsion PCR, and 454 pyrosequencing according to the manufacturer's instructions. After trimming of primer sequences, the reads were clustered and assembled into contiguous fragments (contigs) using Geneious 6 (67). Consensus sequences and unassembled reads (nucleotide and translated amino acid sequences) were compared to the GenBank database using Basic Local Alignment Search Tool (BLASTn, BLASTp, BLASTx, and tBLASTx). Reads and contigs that showed simi-

larity to viral sequences were reference mapped to all reads with iterations up to five times.

Genome sequencing and analysis. Sequence contigs obtained by 454 pyrosequencing were confirmed with standard PCR with Platinum *Taq* DNA polymerase (Life Technologies) and contig-specific primers. The 5′ and 3′ genome termini were analyzed by rapid amplification of cDNA ends (RACE) (Life Technologies). RACE PCR products were cloned into the TopoTA pCR4 cloning vector (Life Technologies) and Sanger sequenced (SeqLab). Sequences were analyzed using Geneious 6 (67). The complete genome was confirmed by long-range PCR and Sanger sequencing on both strands. The 5′ ends of the subgenomic mRNAs were amplified with gene-specific primers for ORF2 and -3 from RNA 1 using the GeneRacer kit (Life Technologies) according to the manufacturer's instructions. Products were sequenced and analyzed using Geneious 6 (67).

Phylogenetic analysis. Amino acid sequences of RdRp and capsid proteins were aligned using MAFFT (68) and the E-INS-I algorithm in Geneious 6 (67). Phylogenetic analyses were conducted by using the maximum likelihood (ML) algorithm with the Dayhoff substitution model, four gamma categories, and no optimization with 1,000 bootstrap replicates using MEGA v5 (69).

RNA analyses. Northern blot analyses of viral RNAs were performed as described previously (3). Briefly, C6/36 cells were infected with MoNV and harvested at 24 hpi. RNA was extracted using the RNeasy minikit (Qiagen) and analyzed by Northern blotting with digoxigenin (DIG)-labeled probes. Probes for protein A (ORF1, RNA 1), protein B2 (ORF3, RNA 1), and the capsid protein (ORF1, RNA 2) were generated using the PCR DIG probe synthesis kit (Roche) and the gene-specific primer pairs MoNV-A-F (5′-GGTGGTCAGCAACGAGTGAA-3′) and MoNV-A-R (5′-TTGTGGCTGCTTCCTTGTCA-3′), MoNV-B2-F (5′-AGAAAATC AGCAGCAACTTCGG-3′) and MoNV-B2-R (5′-TCACTTCGCTTCGA CGATGG-3′), and MoNV-C-F (5′-CCGGATACAACATCGACGACCC C-3′) and MoNV-C-R (5′-ACTCGCGACAGGTTTGATGACACT-3′), respectively.

Plasmids. The following plasmids were described previously: pMT-Luc and pMT-Ren (48), pAWH-CrPV1A (32, 58), and pAc-DXV VP3 (57). To clone MoNV B2 into an insect expression plasmid, total RNA was isolated from MoNV-infected C6/36 cells using Isol-RNA lysis reagent (5 Prime) and reverse transcribed into cDNA using TaqMan reverse transcription reagents (Roche) and random hexamers (Roche). The MoNV B2 ORF was PCR amplified using the primers 5′-ACGTGGTACCCAAA ATGACAGAAAATCAGCAGCAACTTC-3′ and 5′-ACGTGCGGCCGC CACTTCGCTTCGACGATGGGGGGC-3′. PCR products were cloned into the Acc65I and NotI restriction sites of pAc5.1-V5-His-Ntag (47). To detect expression of V5-tagged MoNV protein, Western blotting was performed using a monoclonal mouse anti-V5 antibody (Invitrogen) and IRDye 680 goat anti-mouse IgG (Li-Cor Biosciences) for detection on the Odyssey infrared imager (Li-Cor Biosciences).

To generate bacterial expression plasmids, MoNV B2 was PCR amplified using the primers 5′-ACGTGGATCCATGACAGAA AATCAGCAG-3′ and 5′-ACGTAAGCTTTCACTTCGCTTCGACGATG G-3′ and cloned into the BamHI and HindIII restriction sites of pMal-C2X (New England BioLabs).

RNAi reporter assays. RNAi reporter assays were performed as described earlier (47, 57, 70). Briefly, for double-stranded-RNA (dsRNA) feeding assays, S2 R+ cells were seeded, and pMT-Luc, pMT-Ren, and VSR expression plasmids were transfected the next day. Three days after transfection, dsRNA targeting firefly luciferase (FLuc) or, as a nonsilencing control, GFP was added to the culture medium to a final concentration of 20 ng/μl. Expression of the reporters was induced with 0.5 mM $CuSO_4$, and luciferase reporter activity was quantified using the dual-luciferase reporter system (Promega). Sequential transfection of siRNAs in S2 cells was described previously (57). S2 cells were seeded at a density of 2.5×10^5 cells per well in a 24-well plate, and 1 day later, 300 ng of VSR expression plasmid or control vector along with 100 ng of pCo-BLAST (Life technologies) was transfected using the transfection reagent Effectene (Qiagen). After 48 h, the cells were split 1:5 and transferred to a 96-well plate in blasticidin-containing Schneider's medium (final concentration of 25 μg/ml) to select for VSR-expressing cells and 1 day thereafter transfected with siRNA targeting Fluc (version GL3; Dharmacon) or negative-control siRNA (Qiagen) along with an empty carrier plasmid (pAc5.1-V5-His-Ntag) using Effectene. Expression of the reporter plasmids was induced with $CuSO_4$ 1 day after the second transfection, and luciferase activities were measured the day after.

For RNAi reporter assays in infected mosquito cells, U4.4 cells were seeded at a density of 1×10^5 cells per well in a 24-well format. The next day, cells were mock infected or infected with MoNV at an MOI of 10. At 2 dpi, the cells were transfected with 250 ng of pMT-Luc, 250 ng pMT-Ren, and either 10 ng of FLuc or GFP dsRNA (dsRNA-initiated RNAi) or 8.1 μl of a 20 μM stock of siRNA targeting GL3 (Dharmacon) or negative-control siRNA (Qiagen) (siRNA-initiated RNAi) using Xtreme Gene HP reagent (Roche). The same day, expression of the reporter plasmids was induced, and luciferase activity was measured 18 h later.

Production of recombinant mosinovirus B2 in *Escherichia coli*. MBP fusion proteins were purified from *E. coli* as described earlier (47). pMAL-MoNV B2 and pMAL-C2X were transformed into competent BL21 cells. Liquid cultures were grown to an optical density at 600 nm (OD_{600}) of 1.3, and protein expression was induced with IPTG (isopropyl-β-D-thiogalactopyranoside) at a final concentration of 1 mM. Cultures were incubated overnight at 18°C, and recombinant proteins were isolated the next day using amylose resin according to the manufacturer's instructions (New England BioLabs). Purified recombinant proteins were dialyzed against dialysis buffer (20 mM Tris-HCl, 0.5 mM EDTA, 5 mM $MgCl_2$, 1 mM dithiothreitol [DTT], 140 mM NaCl, 2.7 mM KCl) and stored in aliquots in dialysis buffer containing 30% glycerol at −80°C.

Radioactively labeled probes. The siRNA (Let-7 guide [5′-UGAGGU AGUAGGUUGUAUAGU-3′] and Let-7 passenger [5′-UAUACAAC CUACUACCUCUCU-3′]) and blunt dsRNA (F [5′-UAUACAACCUAC UACCUCUCU-3′] and R [5′-UAUACAACCUACUACCUCUCU-3′]) probes were annealed and end labeled using [γ-^{32}P]ATP and polynucleotide kinase (Roche). Unincorporated nucleotides were removed on G-25 Sephadex columns (Roche). Radioactively labeled dsRNA was prepared as described earlier (47, 48).

Electrophoretic mobility shift assays (EMSAs). Gel mobility shift assays were performed as described before (47, 48). Briefly, ^{32}P end-labeled 21-nt siRNA duplexes and 21-nt blunt dsRNA (both at a final concentration of 1 nM per reaction) or uniformly ^{32}P-labeled 126-nt dsRNA (5 ng per reaction) were incubated with different concentrations of purified recombinant proteins in binding buffer (5 mM HEPES, 25 mM KCl, 2 mM $MgCl_2$, 3,8% glycerol) and 10 mg/ml tRNA (Roche) for 60 min at room temperature. EMSAs with 21-nt siRNA and blunt dsRNA were analyzed on an 8% native polyacrylamide gel at 4°C, whereas EMSAs with 126-nt labeled dsRNAs were analyzed on a 6% native gel. Radioactive gels were imaged by exposure to Kodak Biomax XAR films.

Dicer assay. Dicer assays were performed as described before (47, 57). Briefly, U4.4 cell lysates were prepared using 30 mM HEPES-KOH (pH 7,4), 100 mM potassium acetate (KOAc), 2 mM $Mg(OAc)_2$, 5 mM DTT, 1× protease inhibitor (Roche). Uniformly ^{32}P-labeled 126-nt dsRNA (5 ng per reaction) was incubated with MoNV-infected U4.4 cell lysate, non-infected cell lysate, and mixtures thereof in different proportions for 3 h at 28°C. Samples were then deproteinized using proteinase K (Life Technologies), extracted with phenol-chloroform, precipitated in the presence of glycogen (Life Technologies), resuspended in loading buffer II (Life Technologies), and analyzed on a 12% polyacrylamide–7 M urea gel.

Nucleotide sequence accession numbers. MoNV sequences were deposited in GenBank under the accession numbers KJ632942 and KJ632943.

RESULTS

Mosinovirus contains a bipartite genome. Mosquitoes were sampled in a survey of mosquito-associated viruses in and around

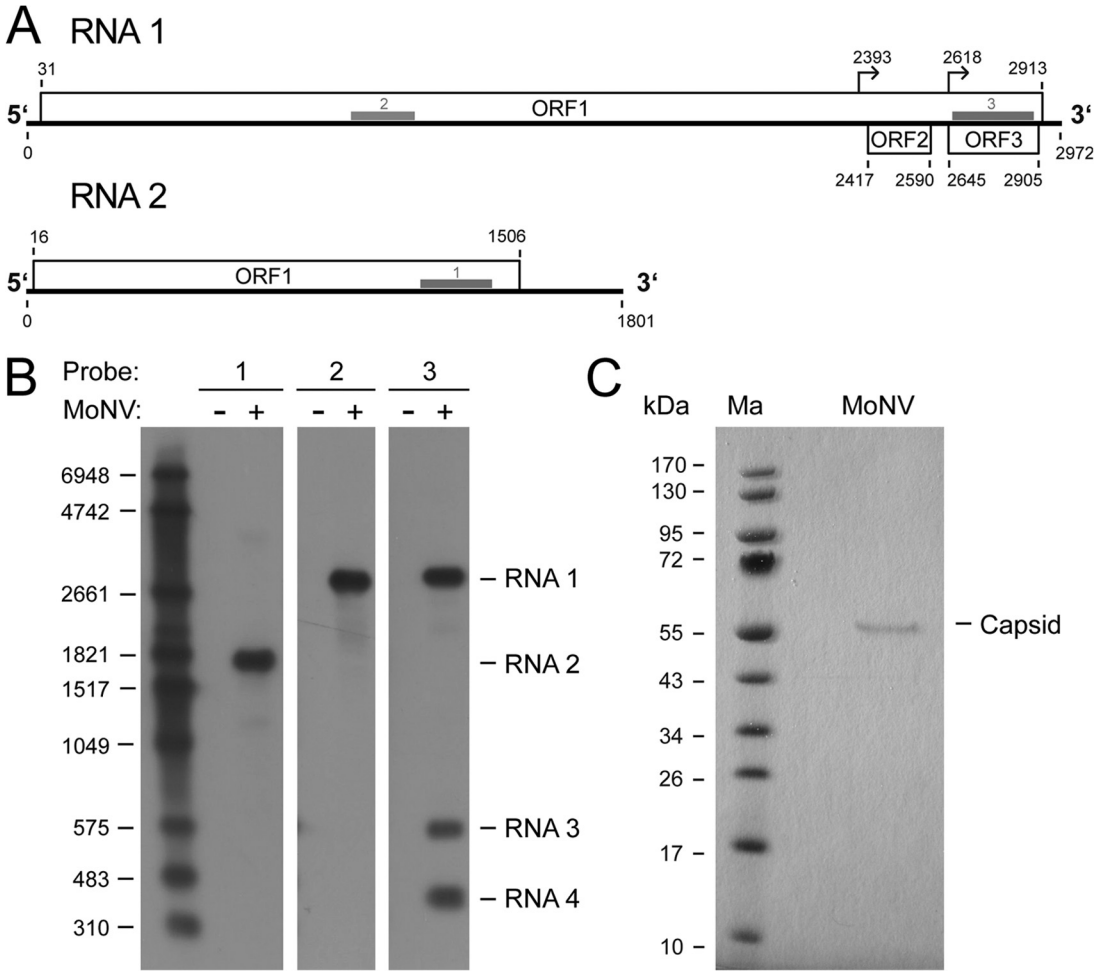

FIG 1 Genome organization, viral transcripts, and structural proteins of MoNV. (A) Schematic organization of the two genome segments. Open reading frames (ORF) are shown by boxes, and sizes of ORFs are indicated by nucleotide positions. Specific probes for Northern blot analyses are shown by gray bars and numbered 1 to 3. Genome positions of the subgenomic RNAs are indicated by arrows. (B) Northern blot analysis of viral RNA isolated from MoNV-infected C6/36 cells at 1 dpi (+). Specific DIG-labeled probes (1 to 3) were used for detection. RNA from uninfected C6/36 cells (−) was used as a mock control. A DIG-labeled RNA was used as a size marker, and sizes (in nucleotides) are on the left. (C) SDS-PAGE analysis of MoNV major structural proteins. Virus particles from cell culture supernatants of infected C6/36 cells were purified by gradient ultracentrifugation. Proteins were stained with Coomassie blue R-250. A molecular mass marker with corresponding sizes is shown on the left.

the Taï National Park, Côte d'Ivoire (64), and MoNV was subsequently isolated from a pool of 4 *Culicidae* sp. mosquitoes (MoNV/C36/CI/2004) in C6/36 cells. Among the 116 mosquito pools that induced CPE in C6/36 cells, we detected MoNV replication by specific real-time RT-PCR in two further pools consisting of 2 *Culex nebulosus* (MoNV/C37/CI/2004) mosquitoes and 4 *Culex* sp. mosquitoes (MoNV/D25/CI/2004). Growth of MoNV was investigated on the vertebrate cell lines Vero E6 and BHK-J. Cells were infected at MOIs of 0.01 and 0.11, and viral genome copies in the cell culture supernatants were measured at 1 hpi and 7 dpi. The number of viral genome copies decreased over time (data not shown), suggesting that MoNV is an insect-specific virus.

Virions of pooled MoNV/C36/CI/2004 were concentrated via ultracentrifugation and prepared for next-generation sequencing. Two separate contigs of 2.964 kb and 363 nt were generated by *de novo* assembly. Initial comparisons of the large and small contigs to the public database (BLASTp, GenBank, NCBI) yielded low but significant similarities to the RdRp protein of members of the family *Nodaviridae* (query coverage, 14 to 93%; E value, 1e-23 - 0.0; identity, 28 to 44%) and to the capsid protein of the monopartite LSV (query coverage, 56 to 66%; E value, 0.37 - 0.003; identity, 32 to 34%), respectively. Attempts to combine these two contigs with specific primers by PCR failed, suggesting that the MoNV genome is segmented. This was confirmed by Northern blotting (see below). The termini of the two genome segments were determined using 5′ and 3′ RACE PCR, and the sequences of both RNA strands were confirmed by specific PCR and Sanger sequencing.

The entire genome of MoNV comprised 2,972 nt (RNA 1) and 1,801 nt (RNA 2). RNA 1 contains in positive-sense orientation three overlapping ORFs of 2,883 nt (ORF1), 174 nt (ORF2) and 261 nt (ORF3) (Fig. 1A). Maximal pairwise identity of 43% of the amino acid sequence of ORF1 was found to the RdRp of Pariacoto virus (PaV) suggesting that ORF1 encodes the MoNV RdRp. We were unable to identify proteins with homology to MoNV ORF2-

and ORF3-encoded proteins among the nonredundant protein sequence database using BLAST searches. RNA 2 contains one ORF of 1,491 nt (496 amino acids [aa]). The highest pairwise identity found, 16%, was to the capsid protein of LSV2, suggesting that RNA 2 encodes the MoNV capsid protein. Like LSV2, the C-terminal part of the putative capsid protein showed similarity to the peptidase family A21 (Pfam PF03566). In contrast, the capsid protein of nodaviruses showed similarity to the peptidase family A6 (Pfam PF01829).

Mosinovirus acquired its capsid gene from a virus beyond the family level. To deduce the evolutionary history of MoNV, we performed phylogenetic analyses based on the deduced amino acid sequences of the RdRp and capsid proteins. Based on the RdRp phylogeny, MoNV clustered in a clade that comprises PaV, WhNV, and HzAM1-derived virus (HzNV) within the family *Nodaviridae*, suggesting that MoNV is a novel nodavirus species (Fig. 2A). Unexpectedly, in phylogenetic analyses based on capsid proteins, MoNV branched from a deep node that shared the most recent common ancestor with LSV1 and LSV2 (Fig. 2B). Given the extreme divergence of the capsid protein sequences, it was not possible to generate sufficiently resolved phylogenetic trees that include all nodavirus species in the analysis. However, maximum likelihood analyses using only the capsid protein sequences of representative nodaviruses showed that MoNV significantly branched from a deep node together with LSV1 and LSV2 (Fig. 2C). Notably, MoNV is placed between the monopartite LSV and the bipartite CBPV. These analyses suggest either that MoNV is a nodavirus that acquired its capsid protein from a virus with a distant relationship to LSV or that MoNV belongs to an unclassified virus family that acquired its RdRp and RNAi inhibitor protein (see below) from nodaviruses. It is widely accepted to investigate the origin and evolution of viruses based on the relationships of their replicative genes and to classify viruses based on these genes (71–73). According to this classification system, the phylogenetic data suggest that MoNV is a novel member of the family *Nodaviridae* that most likely acquired its capsid gene via reassortment from an unknown virus beyond the family level. In contrast to this widely applied classification system, nodaviruses are classified on the basis of, besides virion and genome organization, the genetic relationship of their capsid genes (20). To aid in taxonomic classification, we next investigated morphological and molecular characteristics of MoNV that are relevant for virus classification.

Morphology and structural proteins of mosinovirus. To analyze virion morphology, we purified MoNV by ultracentrifugation over a sucrose cushion and analyzed virions by negative staining electron microscopy. Like nodaviruses, virions were nonenveloped and icosahedral. However, the diameter of MoNV virions was 50 nm, which is much larger than other nodaviruses (Fig. 3A). This larger virion size might be determined by the capsid protein, which is only distantly related to capsids of members of the family *Nodaviridae* (Fig. 2). Analysis of the capsid protein of purified MoNV virions showed a single protein of ~56 kDa (Fig. 1C). The molecular mass was slightly higher than the predicted mass of the protein product of ORF1 of RNA 2 (53.2 kDa), suggesting that the mature MoNV capsid protein does not depend on cleavage from a precursor protein.

Mosinovirus produces two distinct subgenomic RNAs. To analyze the viral RNAs that are produced during infection, we performed Northern blot analyses on total RNA extracted at 1 dpi from infected and noninfected C6/36 cells using specific probes for RNA 1 and RNA 2. For RNA 1, we used two probes that hybridize in different genomic regions. The first probe was placed in the RdRp-coding ORF1 (Fig. 1A). The second probe was placed at the 3′ end of RNA 1 in ORF3 to analyze if ORF2 and ORF3 are expressed as subgenomic RNAs. As expected, one band of approximately 1.8 kb was observed for RNA 2, and one band of ~2.9 kb was detected using the probe specific for the putative RdRp ORF (Fig. 1B, + lanes). These bands were specific, as no signal was observed in RNA from noninfected cells (Fig. 1B, lanes −). Using the probe for the 3′ region of RNA 1, we detected three distinct RNAs: the 2.9-kb full-length RNA 1, as well as two additional subgenomic RNAs (RNA 3, of ~600 nt, and RNA 4, of ~350 nt) of approximately the same intensity (Fig. 1B). To determine the transcription start site of the subgenomic RNAs, we performed specific 5′ RACE on the capped mRNA from infected cells using specific primers for ORF2 and -3. Analysis of sequenced clones suggested that subgenomic RNA 3 starts at genome position 2393 with the sequence 5′-GTGAAGAGAC, whereas subgenomic RNA 4 begins further downstream at position 2618 with the sequence 5′-GTGTAATCGC (Fig. 1A). These transcription start sites of the subgenomic RNAs are located 24 and 27 nt upstream of the start-codon of the potential ORF2 and -3, respectively. Our data indicate that MoNV expresses two distinct subgenomic capped RNAs, predicted to encode 6.8- and 9.8-kDa proteins.

Mosinovirus suppresses RNAi. MoNV was initially isolated in the Dicer-2-defective *Aedes albopictus* C6/36 cell line and grows to a titer of 4×10^6 $TCID_{50}$/ml in these cells. We thus compared viral growth in C6/36 cells to that in the RNAi-competent U4.4 cell line derived from the same mosquito species. C6/36 cells infected with MoNV showed stretching and aggregation of cells at three dpi (Fig. 3B). CPE of MoNV in U4.4 cells was similar but less pronounced at that time point and did not increase at 5 dpi (Fig. 3C). CPE of MoNV in U4.4 was observed daily until 8 dpi but did not increase further. Viral RNA in the supernatants of both cell lines was measured by real-time RT-PCR over a period of 5 days. Concentrations of genome copies increased approximately 1,000-fold in both cell lines within the first 24 hpi (Fig. 3D). From day 2 to 5, the increase of viral RNA concentrations was between 100- and 10-fold lower in U4.4 cells than C6/36 cells, suggesting that MoNV is targeted by the mosquito RNAi machinery. We thus hypothesized that MoNV evolved mechanisms to suppress or evade the antiviral RNAi machinery to ensure efficient replication.

We used a well-established RNAi reporter assay to determine if MoNV inhibits the RNAi pathway in mosquito cells (47, 57, 70). To this end, we analyzed how MoNV infection affects the efficiency of RNAi-mediated silencing of a firefly luciferase (FLuc) reporter in U4.4 cells. We transfected mock- or MoNV-infected U4.4 cells with a FLuc reporter plasmid along with dsRNA targeting FLuc (dsFLuc), as well as a *Renilla* luciferase (RLuc) expression plasmid for normalization purposes. The FLuc reporter was efficiently silenced (~80-fold) in mock-infected cells. In MoNV-infected cells, however, silencing of FLuc was reduced ~10-fold, suggesting that MoNV suppresses dsRNA-induced RNAi (Fig. 4A). To bypass Dcr-2-dependent cleavage of dsRNA into siRNAs, we induced RNAi by transfection of siRNAs (siFLuc) along with the reporter plasmids. In mock-infected cells, the FLuc reporter was efficiently silenced (~10-fold), but MoNV infection completely abolished RNAi-mediated silencing (Fig. 4B). These results

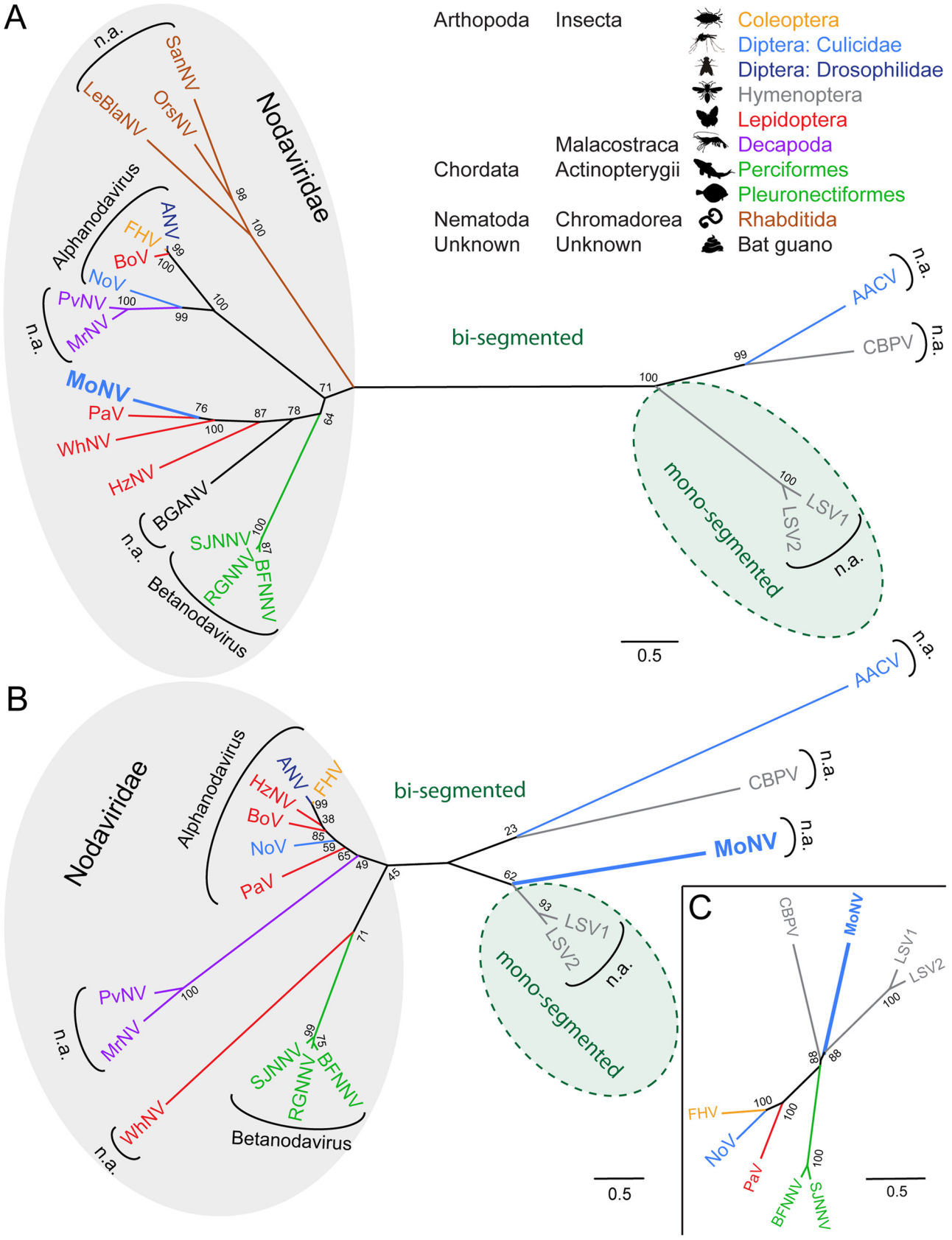

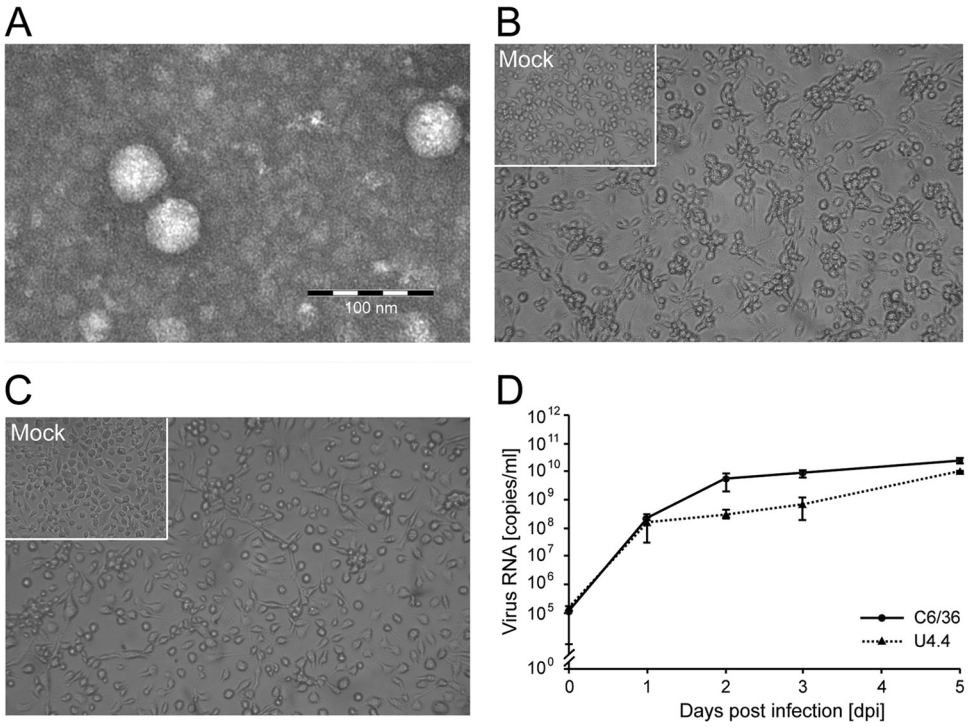

FIG 3 Morphology and growth of MoNV. (A) Morphology of MoNV virions. Viral particles from C6/36 infected-cell-culture supernatants were purified by ultracentrifugation through a 36% sucrose cushion and analyzed by negative-stain electron microscopy. (B) Cytopathic effects of C6/36 cells at 4 days postinfection (dpi) with MoNV. (C) Cytopathic effects of U4.4 cells at 5 dpi. (D) Growth of MoNV in C6/36 and U4.4 cells. Cells were infected at an MOI of 0.001 $TCID_{50}$ per cell in two independent replicates. Genome copies per milliliter of cell culture supernatant were measured by specific RT-PCR at the indicated time points postinfection.

indicate that MoNV is able to suppress the host RNAi response induced by long dsRNA as well as siRNAs.

Mosinovirus B2 protein inhibits RNAi. Nodaviruses encode on their subgenomic RNA 3 the B2 protein, which was shown to function as a potent VSR for some family members (30, 31, 74–76). MoNV expresses two subgenomic RNAs, RNA 3 and RNA 4, which are predicted to encode 6.8- and 9.8-kDa proteins, respectively (Fig. 1 and 4). No significant identity or similarity exists between these predicted proteins and the VSRs of other nodaviruses. We thus analyzed whether either subgenomic RNA encodes a VSR that would explain the RNAi-suppressive activity in infected cells. We generated expression plasmids encoding V5 epitope-tagged ORF2- and ORF3-encoded proteins. Expression of the ORF3-encoded protein was confirmed by Western blotting, but we were unable to stably express the ORF2-encoded protein (data not shown). We thus tested whether the MoNV ORF3-encoded protein suppresses RNAi using reporter assays in *Drosophila* S2 cells. We observed that FLuc was silenced (~11-fold) in cells that were transfected with the vector control (Fig. 4C). However, RNAi-mediated silencing of FLuc was abolished in cells expressing MoNV ORF3. The positive control, the cricket paralysis virus 1A protein (CrPV 1A) (32, 58), suppressed RNAi to a similar extent. Based on these results and results from biochemical assay (discussed below), we propose that ORF3 encodes a MoNV B2-like RNAi suppressor.

Next, we performed an RNAi reporter assay in which FLuc was silenced by sequence-specific siRNA. In this assay, FLuc expression was efficiently silenced (>100-fold), both in control cells and in cells expressing MoNV B2, suggesting that B2 does not suppress siRNA-initiated RNAi (Fig. 4D). In contrast, the positive control Nora virus VP1, which suppresses AGO2-mediated Slicer activity (47, 59), efficiently abolished RNAi-mediated silencing. Our re-

FIG 2 Phylogenetic relationship of MoNV. Phylogenies were investigated for the RdRp (A) and the capsid protein, including all nodaviruses (B) or representative nodaviruses only (C). Maximum likelihood (ML) analyses were performed on all sites of an alignment guided by the Dayhoff substitution matrix using MEGA v5. Bootstrap values are given at nodes and are based on 1,000 bootstrap replicates. Bars indicate evolutionary substitutions. The virus-host associations are highlighted by color and represented by symbols in the top right corner. Members of the family *Nodaviridae* are shaded in gray. The monosegmented viruses LSV1 and LSV2 are shaded in green. Abbreviations and GenBank accession numbers (in parentheses) for RNA 1 and 2 are as follows: AACV, anopheline-associated C virus (KF298264, KF298265); ANV, *Drosophila melanogaster* American nodavirus (GQ342965, GQ342966); BFNNV, barfin flounder nervous necrosis virus (NC_013458, NC_013459); BGANV, bat guano-associated nodavirus (HM228873); BoV, Boolarra virus (NC_004142, NC_004145); CBPV, chronic bee paralysis virus (NC_010711, NC_010712); FHV, Flock House virus (NC_004146, NC_004144); HzNV, HzAM1-derived virus (GU976287, GU976286); LeBlaNV, Le Blanc nodavirus (JQ943579); LSV1, Lake Sinai virus 1 (HQ871931); LSV2, Lake Sinai virus 2 (HQ888865); MoNV, mosinovirus (KJ632942, KJ632943); MrNV, *Macrobrachium rosenbergii* nodavirus (NC_005094, NC_005095); NoV, nodamura virus (NC_002690, NC_002691); OrsNV, Orsay nodavirus (HM030970); PaV, Pariacoto virus (NC_003691, NC_003692); PvNV, *Penaeus vannamei* nodavirus (NC_014978, NC_014977); RGNNV, red-spotted grouper nervous necrosis virus (NC_008040, NC_008041); SanNV, Santeuil nodavirus (NC_015069); SJNNV, striped jack nervous necrosis virus (NC_003448, NC_003449); WhNV, Wuhan nodavirus (AY962576, DQ233638).

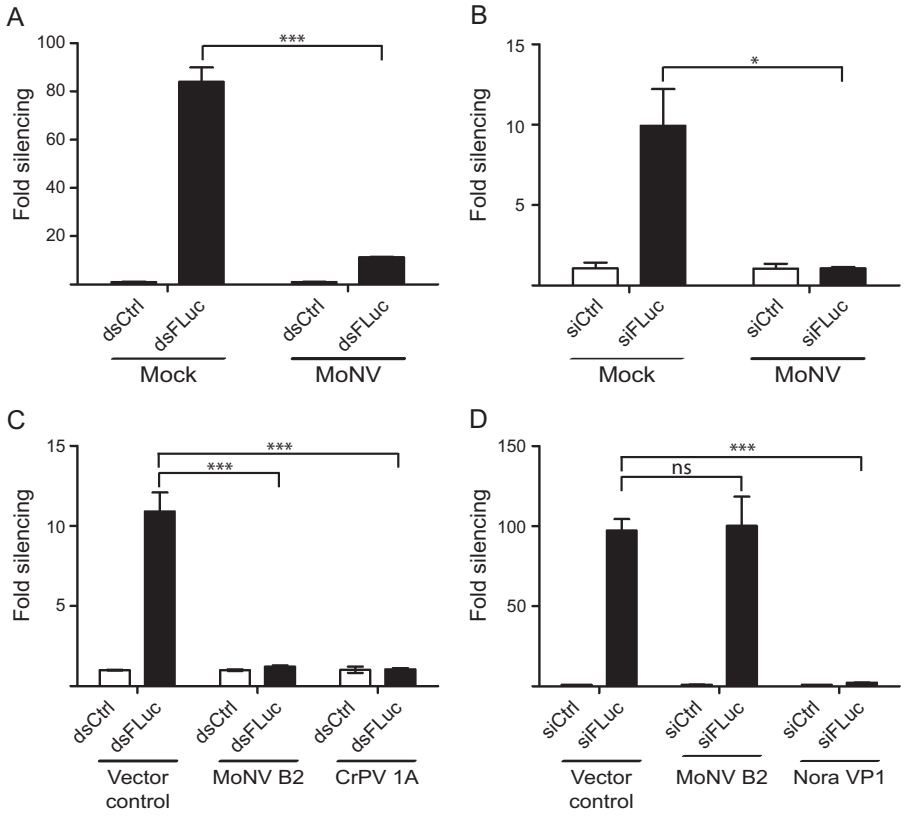

FIG 4 MoNV B2 suppresses RNAi. (A) dsRNA-initiated RNAi reporter assay in mock- or MoNV-infected U4.4 cells. Cells were mock infected or infected with MoNV (MOI = 10) and transfected at 48 hpi with reporter plasmids encoding firefly luciferase (FLuc) and *Renilla* luciferase (RLuc) along with FLuc-specific dsRNA (dsFLuc) or nonspecific control dsRNA (dsCtrl). (B) siRNA-initiated RNAi reporter assay in mock- or MoNV-infected U4.4 cells. FLuc expression was silenced by transfection of FLuc-specific siRNA (siFLuc) or control siRNA (siCtrl) along with FLuc and RLuc reporter plasmids. (C) dsRNA-initiated RNAi reporter assay in S2 R+ cells expressing MoNV B2 or CrPV 1A or in cells transfected with empty control vector, as indicated. RNAi was induced by addition of dsFLuc or dsCtrl to the culture supernatant at 48 h after transfection. (D) siRNA-initiated RNAi reporter assay in S2 R+ cells expressing MoNV B2 or Nora virus VP1 or in cells transfected with empty control vector as indicated. RNAi was induced by transfection of siFLuc or siCtrl at 72 h after transfection of luciferase reporter plasmids and plasmids encoding the VSRs. Firefly luciferase counts were normalized using *Renilla* luciferase counts, and data are expressed as silencing (fold) compared to dsCtrl (A and C) or siCtrl (B and D). Data are means and standard deviations (SD) for 3 biological replicates. *, $P < 0.05$; ***, $P < 0.005$ (Student's *t* test). NS, not significant.

sults therefore indicate that MoNV B2 inhibits the RNAi pathway at a step before RISC-mediated target RNA cleavage. Unexpectedly, we observed that siRNA-initiated RNAi is suppressed in infected cells but not in cells expressing B2 protein from a plasmid (compare Fig. 4B to Fig. 4D), suggesting that another factor in MoNV-infected cells is required for suppression of siRNA-initiated RNAi.

Mosinovirus B2 possesses dsRNA binding activity. Viral RNAi antagonists may target different steps in the RNAi pathway, including Dicer-mediated processing of dsRNA, incorporation of siRNA into RISC, or RISC-mediated cleavage of target RNA (34, 77). To determine whether MoNV B2 binds dsRNA, we performed electrophoretic mobility shift assays (EMSAs) using recombinant maltose-binding protein (MBP)-tagged MoNV B2 protein. Binding of B2 to dsRNA in a dose-dependent manner was observed (Fig. 5A, lanes 3 to 12). B2 completely shifted the dsRNA at concentrations of 5 μM and higher (Fig. 5A, lanes 3 and 4), whereas a partial shift was observed at concentrations ranging from 156 nM to 2.5 μM (Fig. 5A, lanes 5 to 9). As expected, no shift in dsRNA mobility was observed in the presence of MPB alone (Fig. 5A, lane 2).

We next analyzed binding of MoNV B2 to 21-nt siRNA by EMSA. We observed inefficient binding of MoNV B2 protein to siRNA, with only a partial shift at the highest concentration tested (21.5 μM) (Fig. 5B, lane 1) but not at lower concentrations (lanes 2 to 4). To analyze whether siRNA binding depends on the 3′ terminal overhang, we analyzed 21-nt blunt dsRNAs by EMSA and observed that MoNV B2 binds blunt 21-nt dsRNA more efficiently than siRNAs, with complete shifts at the highest concentrations of B2 (21.5 μM and 10 μM) (Fig. 5B, lanes 7 and 8) and a partial shift at 2.5 μM (lane 9). Again, MBP did not shift siRNA or blunt 21-nt dsRNA (Fig. 5B, lanes 5 and 11). Collectively, these results indicate that MoNV B2 efficiently binds long dsRNA, which suggests that B2 interferes with processing of dsRNA by Dcr-2. Moreover, the low affinity of B2 for siRNAs might account for its inability to suppress siRNA-mediated RNAi in reporter assays (Fig. 4D).

Mosinovirus B2 prevents dsRNA cleavage by Dicer. We next tested whether MoNV inhibits Dcr-2-mediated processing of dsRNA into siRNAs in cell extracts. To this end, we prepared U4.4 cell lysates from both MoNV-infected and mock-infected cells. As reported before (78), radiolabeled dsRNA was readily processed in

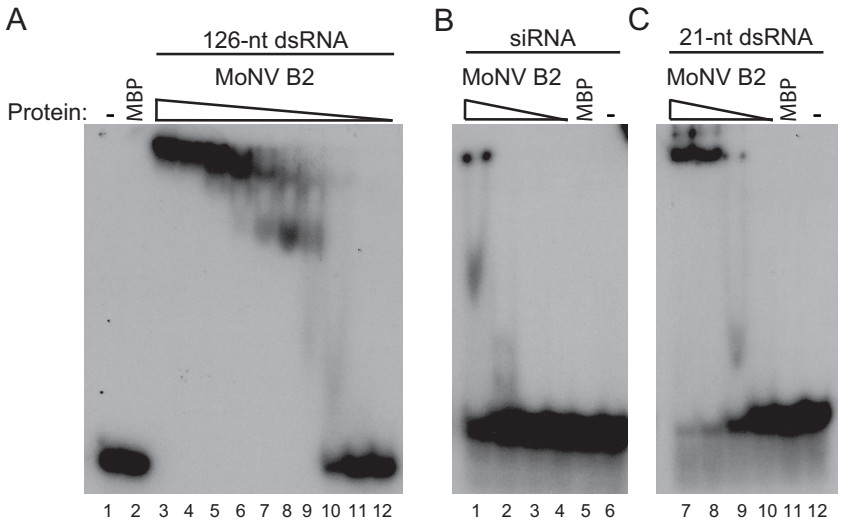

FIG 5 MoNV B2 binds long dsRNA and siRNAs. (A) Electrophoretic mobility shift assay (EMSA) with 126-nt dsRNA. Uniformly radiolabeled 126-nt dsRNA was incubated with buffer (lane 1), MBP (10 μM, lane 2), or decreasing concentrations of recombinant MBP-B2 (2-fold dilutions starting at 10 μM [lanes 3 to 12]). (B and C) EMSA with 21-nt siRNA (B) and 21-nt blunt dsRNA (C). Radiolabeled siRNAs (lanes 1 to 6) or 21-nt blunt dsRNA (lanes 7 to 12) were incubated with MBP (10 μM [lanes 5 and 11]), buffer (lanes 6 and 12), or decreasing concentrations of recombinant MBP-B2 (lanes 3 to 6 and 9 to 12). For MBP-B2, the following concentrations were used: 21.5 μM (lanes 1 and 7), 10 μM (lanes 2 and 8), 2.5 μM (lanes 3 and 9), and 0.625 μM (lanes 4 and 10).

extracts from noninfected U4.4 cells (Fig. 6A, lane 5). In contrast, dsRNA processing into siRNAs was inefficient in extracts from MoNV-infected cells (Fig. 6A, lane 1). Titrating the MoNV-infected extract into the noninfected extract resulted in a dose-dependent decrease in processing of dsRNA into siRNAs (Fig. 6A, lanes 2 to 4). These results suggest that MoNV infection prevents processing of dsRNA into siRNAs. We next performed Dicer assays using recombinant MoNV B2 protein to directly analyze whether B2 is responsible for inhibition of dsRNA cleavage by Dcr-2. Indeed, we observed that MoNV B2 was able to efficiently inhibit the processing of dsRNA into siRNAs in a dose-dependent manner (Fig. 6B, lanes 3 to 5).

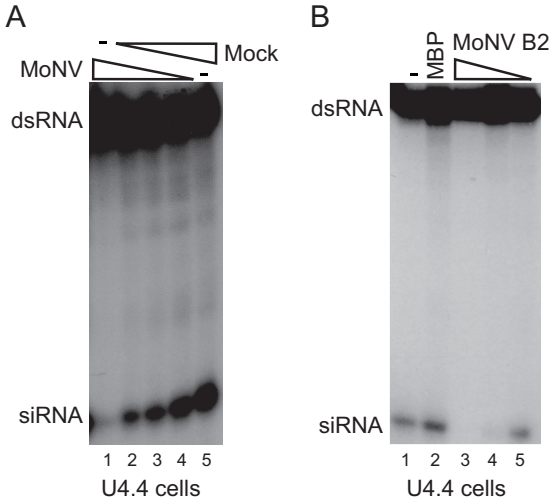

FIG 6 MoNV B2 inhibits Dcr processing of dsRNA. (A) Processing of 126-nt dsRNA in extracts of noninfected or MoNV-infected U4.4 cells. Uniformly radiolabeled dsRNA was incubated in lysate of MoNV-infected U4.4 cells (lane 1), noninfected U4.4 lysate alone (lane 5), or mixtures of mock- and MoNV-infected lysates (lanes 2 to 4, ratios of 3:1, 2:2, and 1:3, respectively). (B) Dicer assay in lysates of U4.4 cells in the presence of decreasing concentrations of MBP-B2 fusion protein (5-fold dilutions starting at 5 μM [lanes 3 to 5]). MBP was used as a negative control (5 μM [lane 2]).

DISCUSSION

In this study, we discovered and characterized a previously unknown virus that was isolated from tropical *Culicidae* mosquitoes. The tentatively named MoNV shares characteristic features with nodaviruses, such as nonenveloped icosahedral virions, a bipartite genome of positive-sense RNA segments of 2.9 and 1.8 kb, similar genome organization, and functions of encoded proteins.

We showed that MoNV encodes two distinct sgRNAs, one encoding a B2-like VSR and the other potentially encoding an ~7-kDa protein with unknown function. No evidence for the expression of more than one subgenomic RNA has been described for nodaviruses, including PaV, the closest relative of MoNV (25). However, the RNA bands of lower mobility that appeared on Northern blots when probes for the subgenomic RNA 3 were used were proposed to be homodimers of sgRNA 3 in other nodaviruses (79, 80).

We demonstrated that ORF3 encodes a potent dsRNA-binding VSR that inhibits the dsRNA-initiated RNAi pathway and inhibits processing of dsRNA into siRNAs by Dicer. Unexpectedly, we observed that siRNA-initiated RNAi is efficiently suppressed in infected cells but not in cells expressing B2 from an expression plasmid. The reason for this discrepancy remains unresolved. Although differences in expression levels in infection versus transfection might account for this difference, our observation that B2 only inefficiently binds siRNAs suggests that another viral factor or interaction of MoNV B2 with other viral proteins is required for suppression of siRNA-initiated RNAi in infected cells.

The mechanism of VSR activity of MoNV B2 is similar to that of B2 proteins of alphanodaviruses and betanodaviruses, including FHV, Nodamura virus (NoV), and greasy grouper nervous necrosis virus (GGNNV), as well as the unclassified WhNV (30,

31, 53, 54, 74–76, 81, 82). Although FHV and NoV B2 share only low sequence identity, these proteins fold into similar structures, consisting of a four-helix bundle capped by two short helices at the C-terminal ends (53, 54, 83). Furthermore, 50% of the 10 amino acid residues interacting with the RNA are identical between FHV and NoV B2 proteins (83), suggesting that these proteins share an ancestor.

The MoNV B2 protein shares only minimal sequence identity to B2 proteins of nodaviruses (27.1% amino acid identity to PaV and 20.5% amino acid identity to WhNV, but the protein does not align to B2 of more distant nodaviruses). Since its position in the genome, its expression strategy, and its mechanism of action seem similar to those of the B2 proteins of other nodaviruses (30, 31, 81, 84, 85), the most parsimonious explanation is that the B2 protein evolved or was present at the nodavirus ancestor. Interestingly, the *Caenorhabditis elegans*-specific nodaviruses do not express an sgRNA or a B2-like VSR (18), indicating that B2 evolved in the ancestor of the alpha, beta, and MoNV clades of nodaviruses.

In phylogenetic analyses based on the RdRp gene, MoNV formed a well-supported sister taxon to Pariacoto virus, suggesting that MoNV is a novel nodavirus species. However, the MoNV capsid protein was not related to nodaviruses, and a maximal pairwise identity of 18% to the capsid proteins of two unclassified viruses with a nonsegmented genome, LSV1 and LSV2, was found. Maximum likelihood analyses of the capsid proteins confirmed this relationship and showed that MoNV shares its most recent common ancestor (MRCA) with LSV1 and LSV2. These widely differing phylogenetic relationships of the MoNV RdRp and capsid proteins complicate its taxonomic classification.

Two hypotheses have been proposed to study the origin and evolution of viruses. The first and most widely accepted hypothesis classifies viruses based on the phylogenetic relationship of their replicative proteins (71, 72). Importantly, replicative proteins are sufficiently conserved to produce reliable alignments and thus to generate robust phylogenetic trees. Furthermore, whereas all RNA viruses encode replicative enzymes, some viruses do not in general encode capsid proteins, others may have lost their capsid proteins during adaption to new hosts, and in others, capsid proteins can be horizontally transferred, which makes virus classification based on capsids impractical (71). The second, more controversial hypothesis proposes that the evolution of viruses is more accurately reflected by the virion architecture and consequently by the relationship of the capsid proteins (86). However, this seems not to be adequate for parsimonious reconstructions of RNA virus evolution (72).

Our results indicate that MoNV shares more characteristics with nodaviruses than with LSV1 and LSV2, suggesting that MoNV is likely an atypical member of the family *Nodaviridae* that acquired its capsid horizontally from a coinfecting LSV-like virus. The coinfected host may have been a bee or a mosquito, as the related LSV and CBPV are both detected in bees and AACV is found in mosquitoes (6–8).

Our data suggest that the capsid protein can be horizontally transferred between viruses of different families. The acquisition of structural proteins from viruses beyond the family level seems to be rare and is limited to viruses that occupy the same ecological niche and infect the same host. Two recently discovered examples include the transfer of a capsid gene from a ssRNA virus (*Tombusviridae*) to an ssDNA virus (circo-like virus) (87, 88) and the transfer of a capsid from parvoviruses to the *Bidnaviridae* (89). Reassortment and recombination were for a long time believed to occur only between genetically closely related viruses that show no more than about 5% distance at the nucleotide level (20, 90–92). Thus, the ability of two viruses to exchange their genome segments serves as a general species demarcation criterion. However, our data and other recent observations (87–89) show that horizontal gene transfer between distantly related viruses plays an important role in viral evolution.

The ICTV classifies nodavirus species on the basis of the phylogenetic relationship of their capsid genes (20). The pairwise identity of the capsid protein to the most closely related species should be less than 80% at the nucleotide level and less than 87% at the amino acid level to classify a virus as a novel species. Thus, the genera *Alphanodavirus* and *Betanodavirus* have been established based on the genetic and phylogenetic relationships of the capsid proteins of their members. Based on this classification system, MoNV would belong to a yet-unknown family. However, it is more likely that MoNV acquired its capsid gene horizontally as outlined above. Such horizontal exchanges of capsid genes seem to be common within the family *Nodaviridae* (Fig. 2A and B). Whereas betanodaviruses form well-supported clades in phylogenetic analyses based on their RdRp and capsid sequences, alphanodaviruses are divided into two different clades in phylogenetic analyses of the RdRp sequences, suggesting that multiple reassortment events have occurred. Consequently, we suggest reclassifying nodaviruses based on the relationship of their RdRp genes, similar to the classification system used for other viral families.

ACKNOWLEDGMENTS

We thank the Ivorian Ministry of Environment and Forest and the Ministry of Research, as well as the directorship of the Taï National Park, for permission to conduct this research. We are grateful to Fabian Leendertz for assistance with fieldwork research design and logistic support. We thank Pascal Trippner and Thierry Kruber for excellent technical assistance.

This work was financially supported by a VIDI fellowship (project number 864.08.003) and the Open Program of the Division for Earth and Life Sciences (project number 821.02.028) from the Netherlands Organization for Scientific Research to R.P.V.R., by a Ph.D. fellowship from the Nijmegen Centre for Molecular Life Sciences to S.S., and by the Deutsche Forschungsgemeinschaft (grant JU 2857/1-1 to SJ and grant VA 827/1-1 to R.P.V.R.) within DFG Priority Programme SPP 1596.

REFERENCES

1. **Zirkel F, Kurth A, Quan PL, Briese T, Ellerbrok H, Pauli G, Leendertz FH, Lipkin WI, Ziebuhr J, Drosten C, and Junglen S.** 2011. An insect nidovirus emerging from a primary tropical rainforest. mBio **2:**e00077-11. http://dx.doi.org/10.1128/mBio.00077-11.
2. **Nga PT, Parquet Mdel C, Lauber C, Parida M, Nabeshima T, Yu F, Thuy NT, Inoue S, Ito T, Okamoto K, Ichinose A, Snijder EJ, Morita K, Gorbalenya AE.** 2011. Discovery of the first insect nidovirus, a missing evolutionary link in the emergence of the largest RNA virus genomes. PLoS Pathog. **7:**e1002215. http://dx.doi.org/10.1371/journal.ppat.1002215.
3. **Zirkel F, Roth H, Kurth A, Drosten C, Ziebuhr J, Junglen S.** 2013. Identification and characterization of genetically divergent members of the newly established family mesoniviridae. J. Virol. **87:**6346–6358. http://dx.doi.org/10.1128/JVI.00416-13.
4. **Marklewitz M, Handrick S, Grasse W, Kurth A, Lukashev A, Drosten C, Ellerbrok H, Leendertz FH, Pauli G, Junglen S.** 2011. Gouleako virus isolated from West African mosquitoes constitutes a proposed novel genus in the family Bunyaviridae. J. Virol. **85:**9227–9234. http://dx.doi.org/10.1128/JVI.00230-11.
5. **Marklewitz M, Zirkel F, Rwego IB, Heidemann H, Trippner P, Kurth A, Kallies R, Briese T, Lipkin WI, Drosten C, Gillespie TR, Junglen S.**

2013. Discovery of a unique novel clade of mosquito-associated bunyaviruses. J. Virol. **87:**12850–12865. http://dx.doi.org/10.1128/JVI.01862-13.
6. **Olivier V, Blanchard P, Chaouch S, Lallemand P, Schurr F, Celle O, Dubois E, Tordo N, Thiery R, Houlgatte R, Ribiere M.** 2008. Molecular characterisation and phylogenetic analysis of chronic bee paralysis virus, a honey bee virus. Virus Res. **132:**59–68. http://dx.doi.org/10.1016/j.virusres.2007.10.014.
7. **Cook S, Chung BY, Bass D, Moureau G, Tang S, McAlister E, Culverwell CL, Glucksman E, Wang H, Brown TD, Gould EA, Harbach RE, de Lamballerie X, Firth AE.** 2013. Novel virus discovery and genome reconstruction from field RNA samples reveals highly divergent viruses in dipteran hosts. PLoS One **8:**e80720. http://dx.doi.org/10.1371/journal.pone.0080720.
8. **Runckel C, Flenniken ML, Engel JC, Ruby JG, Ganem D, Andino R, DeRisi JL.** 2011. Temporal analysis of the honey bee microbiome reveals four novel viruses and seasonal prevalence of known viruses, Nosema, and Crithidia. PLoS One **6:**e20656. http://dx.doi.org/10.1371/journal.pone.0020656.
9. **Bailey L, Newman JF, Porterfield JS.** 1975. The multiplication of Nodamura virus in insect and mammalian cell cultures. J. Gen. Virol. **26:**15–20. http://dx.doi.org/10.1099/0022-1317-26-1-15.
10. **Ball LA, Amann JM, Garrett BK.** 1992. Replication of nodamura virus after transfection of viral RNA into mammalian cells in culture. J. Virol. **66:**2326–2334.
11. **Selling BH, Allison RF, Kaesberg P.** 1990. Genomic RNA of an insect virus directs synthesis of infectious virions in plants. Proc. Natl. Acad. Sci. U. S. A. **87:**434–438. http://dx.doi.org/10.1073/pnas.87.1.434.
12. **Price BD, Eckerle LD, Ball LA, Johnson KL.** 2005. Nodamura virus RNA replication in Saccharomyces cerevisiae: heterologous gene expression allows replication-dependent colony formation. J. Virol. **79:**495–502. http://dx.doi.org/10.1128/JVI.79.1.495-502.2005.
13. **Vendramin N, Toffan A, Mancin M, Cappellozza E, Panzarin V, Bovo G, Cattoli G, Capua I, Terregino C.** 2014. Comparative pathogenicity study of ten different betanodavirus strains in experimentally infected European sea bass, Dicentrarchus labrax (L.). J. Fish Dis. **37:**371–383. http://dx.doi.org/10.1111/jfd.12117.
14. **Bai H, Wang Y, Li X, Mao H, Li Y, Han S, Shi Z, Chen X.** 2011. Isolation and characterization of a novel alphanodavirus. Virol. J. **8:**311. http://dx.doi.org/10.1186/1743-422X-8-311.
15. **Liu C, Zhang J, Yi F, Wang J, Wang X, Jiang H, Xu J, Hu Y.** 2006. Isolation and RNA1 nucleotide sequence determination of a new insect nodavirus from Pieris rapae larvae in Wuhan city, China. Virus Res. **120:**28–35. http://dx.doi.org/10.1016/j.virusres.2005.09.003.
16. **Johnson KN, Zeddam JL, Ball LA.** 2000. Characterization and construction of functional cDNA clones of Pariacoto virus, the first Alphanodavirus isolated outside Australasia. J. Virol. **74:**5123–5132. http://dx.doi.org/10.1128/JVI.74.11.5123-5132.2000.
17. **Zeddam JL, Rodriguez JL, Ravallec M, Lagnaoui A.** 1999. A noda-like virus isolated from the sweetpotato pest spodoptera eridania (Cramer) (Lep.; Noctuidae). J. Invertebrate Pathol. **74:**267–274. http://dx.doi.org/10.1006/jipa.1999.4881.
18. **Felix MA, Ashe A, Piffaretti J, Wu G, Nuez I, Belicard T, Jiang Y, Zhao G, Franz CJ, Goldstein LD, Sanroman M, Miska EA, Wang D.** 2011. Natural and experimental infection of Caenorhabditis nematodes by novel viruses related to nodaviruses. PLoS Biol. **9:**e1000586. http://dx.doi.org/10.1371/journal.pbio.1000586.
19. **Qian D, Shi Z, Zhang S, Cao Z, Liu W, Li L, Xie Y, Cambournac I, Bonami JR.** 2003. Extra small virus-like particles (XSV) and nodavirus associated with whitish muscle disease in the giant freshwater prawn, Macrobrachium rosenbergii. J. Fish Dis. **26:**521–527. http://dx.doi.org/10.1046/j.1365-2761.2003.00486.x.
20. **Thiery R, Johnson KL, Nakai T, Schneemann A, Bonami JR, Lightner DV.** 2012. Family Nodaviridae, p 1061–1067. *In* King AMQ, Adams MJ, Carstens EB, Lefkowitz FJ (ed), Virus taxonomy: ninth report of the International Committee on Taxonomy of Viruses, vol. 9. Elsevier, Amsterdam, The Netherlands.
21. **Gallagher TM, Rueckert RR.** 1988. Assembly-dependent maturation cleavage in provirions of a small icosahedral insect ribovirus. J. Virol. **62:**3399–3406.
22. **Schneemann A, Zhong W, Gallagher TM, Rueckert RR.** 1992. Maturation cleavage required for infectivity of a nodavirus. J. Virol. **66:**6728–6734.
23. **Tang L, Lin CS, Krishna NK, Yeager M, Schneemann A, Johnson JE.** 2002. Virus-like particles of a fish nodavirus display a capsid subunit domain organization different from that of insect nodaviruses. J. Virol. **76:**6370–6375. http://dx.doi.org/10.1128/JVI.76.12.6370-6375.2002.
24. **Liu C, Zhang J, Wang J, Lu J, Chen W, Cai D, Hu Y.** 2006. Sequence analysis of coat protein gene of Wuhan nodavirus isolated from insect. Virus Res. **121:**17–22. http://dx.doi.org/10.1016/j.virusres.2006.03.011.
25. **Johnson KN, Ball LA.** 2001. Recovery of infectious pariacoto virus from cDNA clones and identification of susceptible cell lines. J. Virol. **75:**12220–12227. http://dx.doi.org/10.1128/JVI.75.24.12220-12227.2001.
26. **Johnson KN, Ball LA.** 2003. Virions of Pariacoto virus contain a minor protein translated from the second AUG codon of the capsid protein open reading frame. J. Gen. Virol. **84:**2847–2852. http://dx.doi.org/10.1099/vir.0.19419-0.
27. **Ball LA.** 1995. Requirements for the self-directed replication of flock house virus RNA 1. J. Virol. **69:**2722.
28. **Aliyari R, Wu Q, Li HW, Wang XH, Li F, Green LD, Han CS, Li WX, Ding SW.** 2008. Mechanism of induction and suppression of antiviral immunity directed by virus-derived small RNAs in Drosophila. Cell Host Microbe **4:**387–397. http://dx.doi.org/10.1016/j.chom.2008.09.001.
29. **Han YH, Luo YJ, Wu Q, Jovel J, Wang XH, Aliyari R, Han C, Li WX, Ding SW.** 2011. RNA-based immunity terminates viral infection in adult Drosophila in the absence of viral suppression of RNA interference: characterization of viral small interfering RNA populations in wild-type and mutant flies. J. Virol. **85:**13153–13163. http://dx.doi.org/10.1128/JVI.05518-11.
30. **Li HW, Li WX, Ding SW.** 2002. Induction and suppression of RNA silencing by an animal virus. Science **296:**1319–1321. http://dx.doi.org/10.1126/science.1070948.
31. **Li WX, Li H, Lu R, Li F, Dus M, Atkinson P, Brydon EW, Johnson KL, Garcia-Sastre A, Ball LA, Palese P, Ding SW.** 2004. Interferon antagonist proteins of influenza and vaccinia viruses are suppressors of RNA silencing. Proc. Natl. Acad. Sci. U. S. A. **101:**1350–1355. http://dx.doi.org/10.1073/pnas.0308308100.
32. **Wang XH, Aliyari R, Li WX, Li HW, Kim K, Carthew R, Atkinson P, Ding SW.** 2006. RNA interference directs innate immunity against viruses in adult Drosophila. Science **312:**452–454. http://dx.doi.org/10.1126/science.1125694.
33. **Bronkhorst AW, van Rij RP.** 2014. The long and short of antiviral defense: small RNA-based immunity in insects. Curr. Opin. Virol. **7C:**19–28. http://dx.doi.org/10.1016/j.coviro.2014.03.010.
34. **Ding SW, Voinnet O.** 2007. Antiviral immunity directed by small RNAs. Cell **130:**413–426. http://dx.doi.org/10.1016/j.cell.2007.07.039.
35. **Bronkhorst AW, van Cleef KW, Vodovar N, Ince IA, Blanc H, Vlak JM, Saleh MC, van Rij RP.** 2012. The DNA virus Invertebrate iridescent virus 6 is a target of the Drosophila RNAi machinery. Proc. Natl. Acad. Sci. U. S. A. **109:**E3604–E3613. http://dx.doi.org/10.1073/pnas.1207213109.
36. **Kemp C, Mueller S, Goto A, Barbier V, Paro S, Bonnay F, Dostert C, Troxler L, Hetru C, Meignin C, Pfeffer S, Hoffmann JA, Imler JL.** 2013. Broad RNA interference-mediated antiviral immunity and virus-specific inducible responses in Drosophila. J. Immunol. **190:**650–658. http://dx.doi.org/10.4049/jimmunol.1102486.
37. **Marques JT, Wang JP, Wang X, de Oliveira KP, Gao C, Aguiar ER, Jafari N, Carthew RW.** 2013. Functional specialization of the small interfering RNA pathway in response to virus infection. PLoS Pathog. **9:**e1003579. http://dx.doi.org/10.1371/journal.ppat.1003579.
38. **Mueller S, Gausson V, Vodovar N, Deddouche S, Troxler L, Perot J, Pfeffer S, Hoffmann JA, Saleh MC, Imler JL.** 2010. RNAi-mediated immunity provides strong protection against the negative-strand RNA vesicular stomatitis virus in Drosophila. Proc. Natl. Acad. Sci.U. S. A. **107:**19390–19395. http://dx.doi.org/10.1073/pnas.1014378107.
39. **Sabin LR, Zheng Q, Thekkat P, Yang J, Hannon GJ, Gregory BD, Tudor M, Cherry S.** 2013. Dicer-2 processes diverse viral RNA species. PLoS One **8:**e55458. http://dx.doi.org/10.1371/journal.pone.0055458.
40. **Vodovar N, Goic B, Blanc H, Saleh MC.** 2011. In silico reconstruction of viral genomes from small RNAs improves virus-derived small interfering RNA profiling. J. Virol. **85:**11016–11021. http://dx.doi.org/10.1128/JVI.05647-11.
41. **Brackney DE, Scott JC, Sagawa F, Woodward JE, Miller NA, Schilkey FD, Mudge J, Wilusz J, Olson KE, Blair CD, Ebel GD.** 2010. C6/36 Aedes albopictus cells have a dysfunctional antiviral RNA interference response. PLoS Negl. Trop. Dis. **4:**e856. http://dx.doi.org/10.1371/journal.pntd.0000856.
42. **Hess AM, Prasad AN, Ptitsyn A, Ebel GD, Olson KE, Barbacioru C,**

Monighetti C, Campbell CL. 2011. Small RNA profiling of Dengue virus-mosquito interactions implicates the PIWI RNA pathway in antiviral defense. BMC Microbiol. **11:**45. http://dx.doi.org/10.1186/1471-2180-11-45.
43. **Myles KM, Morazzani EM, Adelman ZN.** 2009. Origins of alphavirus-derived small RNAs in mosquitoes. RNA Biol. **6:**387–391. http://dx.doi.org/10.4161/rna.6.4.8946.
44. **Scott JC, Brackney DE, Campbell CL, Bondu-Hawkins V, Hjelle B, Ebel GD, Olson KE, Blair CD.** 2010. Comparison of dengue virus type 2-specific small RNAs from RNA interference-competent and -incompetent mosquito cells. PLoS Negl. Trop. Dis. **4:**e848. http://dx.doi.org/10.1371/journal.pntd.0000848.
45. **Siu RW, Fragkoudis R, Simmonds P, Donald CL, Chase-Topping ME, Barry G, Attarzadeh-Yazdi G, Rodriguez-Andres J, Nash AA, Merits A, Fazakerley JK, Kohl A.** 2011. Antiviral RNA interference responses induced by Semliki Forest virus infection of mosquito cells: characterization, origin, and frequency-dependent functions of virus-derived small interfering RNAs. J. Virol. **85:**2907–2917. http://dx.doi.org/10.1128/JVI.02052-10.
46. **Li Y, Ball LA.** 1993. Nonhomologous RNA recombination during negative-strand synthesis of flock house virus RNA. J. Virol. **67:**3854–3860.
47. **van Mierlo JT, Bronkhorst AW, Overheul GJ, Sadanandan SA, Ekstrom JO, Heestermans M, Hultmark D, Antoniewski C, van Rij RP.** 2012. Convergent evolution of argonaute-2 slicer antagonism in two distinct insect RNA viruses. PLoS Pathog. **8:**e1002872. http://dx.doi.org/10.1371/journal.ppat.1002872.
48. **van Rij RP, Saleh MC, Berry B, Foo C, Houk A, Antoniewski C, Andino R.** 2006. The RNA silencing endonuclease Argonaute 2 mediates specific antiviral immunity in Drosophila melanogaster. Genes Dev. **20:**2985–2995. http://dx.doi.org/10.1101/gad.1482006.
49. **Deddouche S, Matt N, Budd A, Mueller S, Kemp C, Galiana-Arnoux D, Dostert C, Antoniewski C, Hoffmann JA, Imler JL.** 2008. The DExD/H-box helicase Dicer-2 mediates the induction of antiviral activity in drosophila. Nat. Immunol. **9:**1425–1432. http://dx.doi.org/10.1038/ni.1664.
50. **Campbell CL, Keene KM, Brackney DE, Olson KE, Blair CD, Wilusz J, Foy BD.** 2008. Aedes aegypti uses RNA interference in defense against Sindbis virus infection. BMC Microbiol. **8:**47. http://dx.doi.org/10.1186/1471-2180-8-47.
51. **Sanchez-Vargas I, Scott JC, Poole-Smith BK, Franz AW, Barbosa-Solomieu V, Wilusz J, Olson KE, Blair CD.** 2009. Dengue virus type 2 infections of Aedes aegypti are modulated by the mosquito's RNA interference pathway. PLoS Pathog. **5:**e1000299. http://dx.doi.org/10.1371/journal.ppat.1000299.
52. **Keene KM, Foy BD, Sanchez-Vargas I, Beaty BJ, Blair CD, Olson KE.** 2004. RNA interference acts as a natural antiviral response to O'nyong-nyong virus (Alphavirus; Togaviridae) infection of Anopheles gambiae. Proc. Natl. Acad. Sci. U. S. A. **101:**17240–17245. http://dx.doi.org/10.1073/pnas.0406983101.
53. **Chao JA, Lee JH, Chapados BR, Debler EW, Schneemann A, Williamson JR.** 2005. Dual modes of RNA-silencing suppression by Flock House virus protein B2. Nat. Struct. Mol. Biol. **12:**952–957. http://dx.doi.org/10.1038/nsmb1005.
54. **Lingel A, Simon B, Izaurralde E, Sattler M.** 2005. The structure of the flock house virus B2 protein, a viral suppressor of RNA interference, shows a novel mode of double-stranded RNA recognition. EMBO Rep. **6:**1149–1155. http://dx.doi.org/10.1038/sj.embor.7400583.
55. **Lu R, Maduro M, Li F, Li HW, Broitman-Maduro G, Li WX, Ding SW.** 2005. Animal virus replication and RNAi-mediated antiviral silencing in Caenorhabditis elegans. Nature **436:**1040–1043. http://dx.doi.org/10.1038/nature03870.
56. **Singh G, Popli S, Hari Y, Malhotra P, Mukherjee S, Bhatnagar RK.** 2009. Suppression of RNA silencing by Flock house virus B2 protein is mediated through its interaction with the PAZ domain of Dicer. FASEB J. **23:**1845–1857. http://dx.doi.org/10.1096/fj.08-125120.
57. **van Cleef KW, Van Mierlo JT, Miesen P, Overheul GJ, Fros JJ, Schuster S, Marklewitz M, Pijlman GP, Junglen S, Van Rij RP.** 2014. Mosquito and Drosophila entomobirnaviruses suppress dsRNA- and siRNA-induced RNAi. Nucleic Acids Res. **42:**8732–8744. http://dx.doi.org/10.1093/nar/gku528.
58. **Nayak A, Berry B, Tassetto M, Kunitomi M, Acevedo A, Deng C, Krutchinsky A, Gross J, Antoniewski C, Andino R.** 2010. Cricket paralysis virus antagonizes Argonaute 2 to modulate antiviral defense in Drosophila. Nat. Struct. Mol. Biol. **17:**547–554. http://dx.doi.org/10.1038/nsmb.1810.
59. **van Mierlo JT, Overheul GJ, Obadia B, van Cleef KW, Webster CL, Saleh MC, Obbard DJ, van Rij RP.** 2014. Novel Drosophila viruses encode host-specific suppressors of RNAi. PLoS Pathog. **10:**e1004256. http://dx.doi.org/10.1371/journal.ppat.1004256.
60. **Yanagawa S, Lee JS, Ishimoto A.** 1998. Identification and characterization of a novel line of Drosophila Schneider S2 cells that respond to wingless signaling. J. Biol. Chem. **273:**32353–32359. http://dx.doi.org/10.1074/jbc.273.48.32353.
61. **Singh KR.** 1967. Cell cultures derived from larvae of Aedes albopictus (Skuse) and Aedes aegypti (L). Curr. Sci. **36:**506–508.
62. **Igarashi A.** 1978. Isolation of a Singh's Aedes albopictus cell clone sensitive to Dengue and Chikungunya viruses. J. Gen. Virol. **40:**531–544. http://dx.doi.org/10.1099/0022-1317-40-3-531.
63. **Junglen S, Kopp A, Kurth A, Pauli G, Ellerbrok H, Leendertz FH.** 2009. A new flavivirus and a new vector: characterization of a novel flavivirus isolated from uranotaenia mosquitoes from a tropical rain forest. J. Virol. **83:**4462–4468. http://dx.doi.org/10.1128/JVI.00014-09.
64. **Junglen S, Kurth A, Kuehl H, Quan PL, Ellerbrok H, Pauli G, Nitsche A, Nunn C, Rich SM, Lipkin WI, Briese T, Leendertz FH.** 2009. Examining landscape factors influencing relative distribution of mosquito genera and frequency of virus infection. Ecohealth **6:**239–249. http://dx.doi.org/10.1007/s10393-009-0260-y.
65. **Biel SS, Gelderblom HR.** 1999. Electron microscopy of viruses. Oxford University, Oxford, United Kingdom.
66. **Hayat MA.** 2000. Principles and techniques of electron microscopy: biological applications. Macmillan Press Houndmills, London, United Kingdom.
67. **Kearse M, Moir R, Wilson A, Stones-Havas S, Cheung M, Sturrock S, Buxton S, Cooper A, Markowitz S, Duran C, Thierer T, Ashton B, Meintjes P, Drummond A.** 2012. Geneious Basic: an integrated and extendable desktop software platform for the organization and analysis of sequence data. Bioinformatics **28:**1647–1649. http://dx.doi.org/10.1093/bioinformatics/bts199.
68. **Katoh K, Standley DM.** 2013. MAFFT multiple sequence alignment software version 7: improvements in performance and usability. Mol. Biol. Evol. **30:**772–780. http://dx.doi.org/10.1093/molbev/mst010.
69. **Tamura K, Peterson D, Peterson N, Stecher G, Nei M, Kumar S.** 2011. MEGA5: molecular evolutionary genetics analysis using maximum likelihood, evolutionary distance, and maximum parsimony methods. Mol. Biol. Evol. **28:**2731–2739. http://dx.doi.org/10.1093/molbev/msr121.
70. **van Cleef KW, van Mierlo JT, van den Beek M, van Rij RP.** 2011. Identification of viral suppressors of RNAi by a reporter assay in Drosophila S2 cell culture. Methods Mol. Biol. **721:**201–213. http://dx.doi.org/10.1007/978-1-61779-037-9_12.
71. **Koonin EV, Wolf YI, Nagasaki K, Dolja VV.** 2008. The Big Bang of picorna-like virus evolution antedates the radiation of eukaryotic supergroups. Nat. Rev. Microbiol. **6:**925–939. http://dx.doi.org/10.1038/nrmicro2030.
72. **Koonin EV, Wolf YI, Nagasaki K, Dolja VV.** 2009. The complexity of the virus world. Nat. Rev. Microbiol. **7:**250. http://dx.doi.org/10.1038/nrmicro2030-c2.
73. Reference deleted.
74. **Qi N, Cai D, Qiu Y, Xie J, Wang Z, Si J, Zhang J, Zhou X, Hu Y.** 2011. RNA binding by a novel helical fold of b2 protein from Wuhan nodavirus mediates the suppression of RNA interference and promotes b2 dimerization. J. Virol. **85:**9543–9554. http://dx.doi.org/10.1128/JVI.00785-11.
75. **Qi N, Zhang L, Qiu Y, Wang Z, Si J, Liu Y, Xiang X, Xie J, Qin CF, Zhou X, Hu Y.** 2012. Targeting of dicer-2 and RNA by a viral RNA silencing suppressor in Drosophila cells. J. Virol. **86:**5763–5773. http://dx.doi.org/10.1128/JVI.07229-11.
76. **Sullivan C, Ganem D.** 2005. A virus-encoded inhibitor that blocks RNA interference in mammalian cells. J. Virol. **79:**7371–7379. http://dx.doi.org/10.1128/JVI.79.12.7371-7379.2005.
77. **van Mierlo JT, van Cleef KW, van Rij RP.** 2011. Defense and counter-defense in the RNAi-based antiviral immune system in insects. Methods Mol. Biol. **721:**3–22. http://dx.doi.org/10.1007/978-1-61779-037-9_1.
78. **Vodovar N, Bronkhorst AW, van Cleef KW, Miesen P, Blanc H, van Rij RP, Saleh MC.** 2012. Arbovirus-derived piRNAs exhibit a ping-pong signature in mosquito cells. PLoS One **7:**e30861. http://dx.doi.org/10.1371/journal.pone.0030861.
79. **Albarino CG, Price BD, Eckerle LD, Ball LA.** 2001. Characterization and template properties of RNA dimers generated during flock house virus

RNA replication. Virology **289:**269–282. http://dx.doi.org/10.1006/viro.2001.1125.
80. **Cai D, Qiu Y, Qi N, Yan R, Lin M, Nie D, Zhang J, Hu Y.** 2010. Characterization of Wuhan Nodavirus subgenomic RNA3 and the RNAi inhibition property of its encoded protein B2. Virus Res. **151:**153–161. http://dx.doi.org/10.1016/j.virusres.2010.04.010.
81. **Fenner BJ, Thiagarajan R, Chua HK, Kwang J.** 2006. Betanodavirus B2 is an RNA interference antagonist that facilitates intracellular viral RNA accumulation. J. Virol. **80:**85–94. http://dx.doi.org/10.1128/JVI.80.1.85-94.2006.
82. **Fenner BJ, Goh W, Kwang J.** 2007. Dissection of double-stranded RNA binding protein B2 from betanodavirus. J. Virol. **81:**5449–5459. http://dx.doi.org/10.1128/JVI.00009-07.
83. **Korber S, Shaik Syed Ali P, Chen JC.** 2009. Structure of the RNA-binding domain of Nodamura virus protein B2, a suppressor of RNA interference. Biochemistry **48:**2307–2309. http://dx.doi.org/10.1021/bi900126s.
84. **Johnson KL, Price BD, Eckerle LD, Ball LA.** 2004. Nodamura virus nonstructural protein B2 can enhance viral RNA accumulation in both mammalian and insect cells. J. Virol. **78:**6698–6704. http://dx.doi.org/10.1128/JVI.78.12.6698-6704.2004.
85. **Dasmahapatra B, Dasgupta R, Ghosh A, Kaesberg P.** 1985. Structure of the black beetle virus genome and its functional implications. J. Mol. Biol. **182:**183–189. http://dx.doi.org/10.1016/0022-2836(85)90337-7.
86. **Krupovic M and Bamford DH.** 2009. Does the evolution of viral polymerases reflect the origin and evolution of viruses? Nat. Rev. Microbiol. **7:**250. http://dx.doi.org/10.1038/nrmicro2030-c1.
87. **Diemer GS, Stedman KM.** 2012. A novel virus genome discovered in an extreme environment suggests recombination between unrelated groups of RNA and DNA viruses. Biol. Direct **7:**13. http://dx.doi.org/10.1186/1745-6150-7-13.
88. **Roux S, Enault F, Bronner G, Vaulot D, Forterre P, Krupovic M.** 2013. Chimeric viruses blur the borders between the major groups of eukaryotic single-stranded DNA viruses. Nat. Commun. **4:**2700. http://dx.doi.org/10.1038/ncomms3700.
89. **Krupovic M, Koonin EV.** 2014. Evolution of eukaryotic single-stranded DNA viruses of the Bidnaviridae family from genes of four other groups of widely different viruses. Sci. Rep. **4:**5347. http://dx.doi.org/10.1038/srep05347.
90. **Lukashev AN.** 2005. Role of recombination in evolution of enteroviruses. Rev. Med. Virol. **15:**157–167. http://dx.doi.org/10.1002/rmv.457.
91. **Marshall N, Priyamvada L, Ende Z, Steel J, Lowen AC.** 2013. Influenza virus reassortment occurs with high frequency in the absence of segment mismatch. PLoS Pathog. **9:**e1003421. http://dx.doi.org/10.1371/journal.ppat.1003421.
92. **Webster RG, Bean WJ, Gorman OT, Chambers TM, Kawaoka Y.** 1992. Evolution and ecology of influenza A viruses. Microbiol. Rev. **56:**152–179.